Original Article *Iran J Ped Hematol Oncol. 2025, Vol 15, No 4, 604-620*

Investigating the Immunological Significance of TGFB1 and MDA in ALL TME

Yibei Song MD[1], Wienaldi MD[1*], Maya Sari Mutia MD[1]

1. Universitas Prima Indonesia
*Corresponding author: Dr. Wienaldi, Universitas Prima Indonesia, JI. Sampul No.3, Sei Putih Bar, Kec. Medan Petisah, Kota Medan, Sumatera Utara 20118. Email: wienaldi111@outlook.com. ORCID ID: 0009-0008-2351-8423.

Received: 11 November 2024 **Accepted:** 26 May 2025

Abstract

Background: The tumor microenvironment (TME) in acute lymphoblastic leukemia (ALL) significantly shapes disease progression and therapeutic responses. This study investigates the regulatory role of bone marrow mesenchymal stem cell (BMSC)-released transforming growth factor beta-induced factor homeobox 1 (TGIF1) on myeloid nuclear differentiation antigen (MNDA) expression, immune infiltration, and patient prognosis in ALL.

Materials and Methods: A comprehensive bioinformatics approach analyzed gene expression, protein interactions, and immunological correlations. Differential expression, enrichment analyses, and protein-protein interaction (PPI) networks identified key regulatory genes. The relationship between TGIF1 and MNDA and their immunological impact were assessed through correlation and survival analyses.

Results: Differential analysis identified 424 differentially expressed genes (DGEs). The PPI network and Cox regression highlighted MNDA as a significant gene associated with patient outcomes. High MNDA expression correlated with better survival (P=0.013), and ROC analysis demonstrated its strong prognostic potential (AUC=0.934). GSEA indicated MNDA involvement in immune-related signaling pathways. Immune infiltration analyses linked MNDA expression to seven immune cell types. Additionally, transcription factor TGIF1 positively correlated with MNDA expression, significantly upregulated in healthy BMSCs but downregulated in ALL samples.

Conclusion: BMSC-derived TGIF1 positively regulates MNDA expression, influencing immune infiltration and ALL progression. Targeting the interplay between TGIF1 and MNDA introduces a new molecular strategy for managing ALL.

Keywords: Acute Lymphoblastic Leukemia, Bioinformatics, Bone Marrow Mesenchymal Stem Cells, Myeloid Nuclear Differentiation Antigen, TGFB1

Introduction

Acute lymphoblastic leukemia (ALL), a hematological cancer, originates from the malignant transformation of lymphoid progenitors (1). As one of the most aggressive hematological malignancies, ALL is most commonly diagnosed in childhood (2-4). The disease is marked by chromosomal abnormalities and genetic mutations that impair the normal differentiation and proliferation of lymphoid precursors (5). Beyond the intrinsic genetic alterations, mounting studies highlights the critical role of the tumor microenvironment (TME) in leukemia progression, treatment resistance, and immune evasion (6).

Notably, the infiltration of immune and stromal cells in the bone marrow TME has been strongly associated with the initiation and progression of ALL (7). Therefore, targeting TME-associated molecular interactions may provide new therapeutic strategies for ALL treatment. Myeloid nuclear differentiation antigen (MNDA) is a myeloid cell-specific protein involved in cell differentiation and apoptosis regulation (8, 9). Acute Lymphoblastic Leukemia (AML) patients with reduced MNDA expression exhibit a higher proportion of granulocytes and monocytes (10). Conversely, MNDA overexpression is associated with better outcomes in chronic lymphocytic leukemia (CLL), where it influences the expression of

[Downloaded from ijpho.ssu.ac.ir on 2026-11-25]

[DOI: 10.18502/ijpho.v15i4.19629]

MCL-1 and BCL-2 to promote apoptosis in CLL cells (11). These observations indicate that MNDA may have immunomodulatory functions within the TME of hematologic malignancies.

In this study, transforming growth factor beta-induced factor homeobox 1 (TGIF1) was identified as an upstream transcriptional regulator of MNDA in both bone marrow mesenchymal stem cells (BMSCs) and ALL cells. TGIF1 is known to play roles in hematopoietic cell differentiation and leukemia suppression. Its expression is reduced in blasts from patients with mixed lineage leukemia rearrangement (MLL-r). In contrast, TGIF1 overexpression in MLL-AF9-transformed cells faciliates differentiation and delays leukemia onset (12). Furthermore, TGIF1 suppresses stem cell self-renewal, and its downregulation has been associated with poor long-term survival in acute myeloid leukemia (13). Interestingly, TGIF1 is also expressed in the vascular compartment of chorionic MSCs, suggesting a potential role in MSC-mediated immunoregulation (14). Given the emerging importance of MSCs in hematopoiesis and immune modulation (15), it is hypothesized that BMSCs-derived TGIF1 may regulate MNDA expression, thereby influencing immune cell dynamics and ALL progression.

Although TGIF1 and MNDA have each been implicated in hematological malignancies, their interaction within the ALL tumor microenvironment remains unexplored. This study is the first to propose the TGIF1–MNDA axis as a novel immunoregulatory pathway and potential therapeutic target. TGIF1, a transcriptional repressor of TGF-β signaling, was found to upregulate MNDA, influencing immune cell infiltration (e.g., Tregs, monocytes) and modulating apoptotic pathways (MCL-1/BCL-2). These findings provide insight into immune evasion in ALL and suggest that targeting this axis may improve chemotherapy response and support precision immunotherapy strategies (12).

Materials and Methods

Ethical Statement

This study is a bioinformatics-based retrospective study investigating gene expression, protein interactions, and immunological correlations in the ALL TME. All analyses in this study were conducted using publicly accessible datasets. As no direct involvement of human participants or experimental animals occurred, institutional ethics approval and individual consent were not necessary.

Datasets downloading and processing

The dataset was downloaded from the Gene Expression Omnibus (GEO, NCBI, USA) and the The Cancer Genome Atlas (TCGA, National Cancer Institute, USA). Using GEO database, GSE206172 microarray associated with MSCs was downloaded, including three adipose mesenchymal stem cell (AMSC) samples and three BMSCs samples. RNA sequencing (RNA-seq) data for ALL was retrieved from the TCGA database, encompassing 553 samples from tumors and one from normal tissue. Utilizing the University of California, Santa Cruz (UCSC) Xena database, the RNA-seq data and survival information for ALL tumor samples and RNA-seq data for Genotype-Tissue Expression (GTEx) normal samples were downloaded, including 135 ALL tumor samples, 341 tumor samples in survival information analysis and 337 normal blood samples in GTEx.

Using Perl language, TCGA and GTEx databases were merged, and only the genes annotated in the two databases were retained. The ALL sample data used for screening transcription factors (TFs) were obtained from TCGA database, and those used for the remaining analysis from UCSC Xena database (16).

This article is distributed under the terms of the Creative Commons Attribution-NonCommercial 4.0 International License.

[Downloaded from ijpho.ssu.ac.ir on 2026-11-25]

[DOI: 10.18502/ijpho.v15i4.19629]

Differential analysis

The analysis for differentially expressed genes (DEGs) was executed utilizing the "limma" tool in R, focusing on the GSE206172 microarray and the TCGA and GTEx integrated dataset, with selection parameters of |logFC| over 1 and *p*-value under 0.05. Using the R software "heatmap" package, heatmap of the DEGs was drawn (16).

Classification of TME and acquisition of candidate DGEs

Classification and scoring of stromal and immune cells in the TME were conducted using the "estimate" tool in R software. The division of stromal and immune cells into groups with high and low scores was in light of their respective median values. Differential gene analyses of these two studied cell types were implemented with the help of the R software "limma" package. The intersection of DGEs between stromal and immune cells was carried out with the "VennDiagram" tool in R, which produced a Venn diagram to highlight potential DGEs.

Gene functional enrichment analysis

Through the R software "clusterProfiler" package, GO and KEGG analyses of the candidate DGEs were made. The "enrichplot" package facilitated the creation of bar and bubble plots, showcasing GO enrichment spanning biological processes (BP), cellular component (CC), and molecular function (MF). Meanwhile, the bar, bubble and circle plots of KEGG enrichment analysis were drawn. Using C2.kegg.v2022.1 database from the GSEA4.2.3 software, the gene enrichment of key genes was compared across groups characterized by high and low expressions. Using the "ggplot2" package in R, we visualized the pathways significantly enriched by the key genes, followed by construction of multiple GSEA maps (17).

Establishing networks of protein-protein interactions (PPI)

Through the STRING database, candidate DGEs obtained from the TME were used for PPI analysis (with "species" limited to "human" and confidence level set as 0.7). The number of adjacency nodes of each gene was counted with R software, and the top 55 genes were extracted to plot a histogram.

Univariate COX analysis and receiver operating characteristic (ROC) curve analysis

Through the R software "survival" package, univariate Cox analysis of candidate DGEs was performed and forest plot of the genes with $p < 0.05$ was drawn. The 13 prognosis-related genes obtained from the univariate Cox analysis were intersected with the 55 genes in the PPI network and the Venn plot was drawn to obtain the key genes. Based on the expression of candidate DGEs and status of the samples from the ALL transcriptome data, the ROC was plotted utilizing the R software pROC package to examine the accuracy of the selected key genes (18). A gene's capacity to serve as a biomarker was validated through its area under the ROC curve (AUC).

Differential analysis and survival analysis of single gene

Through the R software "beeswarm" package, a differential expression heatmap of the key genes was drawn. Meanwhile, the key genes were classified into high- and low-expression groups concerning their expression. Through the "survival" and "survminer" packages, survival analysis of the key genes was made.

Immune infiltration analysis

Key genes were stratified into high- and low-expression cohorts concerning their relative transcript abundance. To characterize the immune landscape of ALL samples, CIBERSORT was employed to deconvolute immune cell populations. The algorithm was run with 100 permutations to ensure robustness, and only samples

This article is distributed under the terms of the Creative Commons Attribution-NonCommercial 4.0 International License.

[Downloaded from ijpho.ssu.ac.ir on 2026-11-25]

[DOI: 10.18502/ijpho.v15i4.19629]

yielding results with $p < 0.05$ were obtained. Through the R software "corrplot" package, the results obtained from CIBERSORT calculations were visualized, and the immune cell histogram and correlation plot were drawn (19). Immune cell variability was subjected to differential analysis via "vioplot", while intercellular correlations were visualized through "ggplot2", "ggpubr", and "ggExtra", retaining results with $p < 0.05$. Overlapping immune features from both analyses were integrated via a Venn diagram to pinpoint gene-associated immune subsets (20).

TF co-expression prediction

Through the human TF website, human TF information was obtained. Differentially up-regulated genes in GSE206172 microarray and differentially down-regulated genes in the merged data of TCGA and GTEx were extracted and intersected with human TFs, and a Venn plot was mapped to obtain key TFs. Correlation analysis between each TF and the key gene was performed (21, 22).

Statistical analysis

R software v4.0.1 (R Foundation for Statistical Computing, Vienna, Austria) was employed for data processing. The mean ± standard deviation was used to express the measurement data. The initial step involved conducting tests for normality and variance homogeneity. Unpaired t-tests were used to compare data from two groups that conformed to normal distribution and variance homogeneity, followed by a Tukey post hoc test. Correlations among observed indicators were established through Spearman's correlation analysis. Differences with *p*-values below 0.05 were interpreted as statistical significance.

Results

Bioinformatics analysis for screening key genes in the TME affecting the prognosis of ALL patients

To illuminate molecular mechanisms to improve ALL, key genes were screened by performing differential analysis of immune and stromal cells in the TME applying ALL RNA-seq data. In addition, PPI and single-gene Cox regression analysis of candidate DGEs were performed. Single-gene survival analysis predicted the key genes and survival prognosis of ALL patients. Functional enrichment analysis was implemented to analyze the biological significance of key genes, and their associations with immune cell infiltration were examined through immune infiltration analysis. The bioinformatics analysis process is elucidated in Figure 1. The workflow illustrates the step-by-step bioinformatics pipeline employed in this study, starting from dataset acquisition to differential gene expression analysis, gene functional enrichment, PPI network construction, survival analysis, immune infiltration analysis, and transcription factor prediction.

Differential gene analysis identified 424 common DEGs in two studied cells in the TME of ALL

The ALL-related gene expression dataset was gathered through the UCSC Xena database, including 135 tumor samples. The TME in ALL is composed of immune cells and stromal cell types. The cellular contents of each sample determined their classification into high and low content groups, which were then analyzed for differential gene expression. Differential analysis of stromal cells was performed, with 771 DEGs obtained (Figure 2A). Differential analysis of immune cells was performed, and 828 DEGs were obtained (Figure 2B). The DEGs obtained from stromal cells and immune cells differential analyses were intersected, which finally

This article is distributed under the terms of the Creative Commons Attribution-NonCommercial 4.0 International License.

[Downloaded from ijpho.ssu.ac.ir on 2026-11-25]

[DOI: 10.18502/ijpho.v15i4.19629]

yielded 424 common DEGs (Figure 2C) as candidate DGEs.

GO and KEGG enrichment analyses validated that the candidate DGEs were enriched in the pathways related to ALL development

GO functional analysis and KEGG pathway analysis of candidate DGEs were performed to deeply explore the MF regulated by candidate DGEs. The results of GO functional analysis showed that the candidate DGEs were mainly enriched in positive regulation of cytokine production, leukocyte migration, cell chemotaxis, myeloid leukocyte activation and positive regulation of defense response in BP. Candidate DGEs were mainly enriched in tertiary granule, secretory granule membrane and external side of plasma membrane in CC. Candidate DGEs were mainly enriched in immune receptor activity, cytokine receptor activity, chemokine receptor activity, amide binding, and peptide receptor activity in MF (Figure 3A, B).

The KEGG analysis uncovered that the candidate DGEs were predominantly linked to cytokine-cytokine receptor interaction, neutrophil extracellular trap formation, NOD-like receptor pathway (Figure 3C, D).

The above results proposed that the candidate DGEs were predominantly engaged in promoting leukocyte migration, activation, and the positive modulation of cytokine activities. The candidate DGEs were mainly enriched in the secretory granule membrane and lateral plasma membrane, with MF involved in regulation of immune receptor, cytokine receptor and chemokine activity.

KEGG analysis found that the candidate DGEs were involved in life activities such as neutrophil extracellular trap formation, interactions between cytokines and cytokine receptors, and NOD-like receptor pathway.

MNDA was a key gene in the TME of ALL affecting the prognosis of ALL patients

The candidate DGEs were input into the String database, with the "species" defined as "human", and the confidence level was set to 0.7. The PPI network of candidate DGEs in the TME of ALL was constructed (Figure 4A). The number of adjacency nodes of each gene was counted with R software, and the top 55 genes based on the node adjacency count were selected as the key network genes, followed by delineation of a bar graph (Figure 4B).

To further study the relationship between candidate DGEs and ALL patient prognosis, the survival data and gene expression data of ALL patients from the UCSC dataset were integrated, univariate Cox analysis was performed, and a forest map was drawn (Figure 4C). A total of 13 genes could significantly affect the prognosis of ALL patients, among which 11 genes were high risk genes and 2 genes were low risk genes.

The key genes of PPI network were intersected with the prognosis-related genes of ALL patients, and MNDA (Figure 4D) was obtained. MNDA was the key gene affecting the prognosis of ALL patients in the TME.

The expression of MNDA in ALL samples was evaluated using single-gene differential expression analysis, which revealed a significant downregulation of MNDA compared to normal samples (Figure 5A). Survival analysis (Kaplan-Meier) unveiled that patients with diminished MNDA levels faced significantly worse outcomes than those with higher expression ($p = 0.013$) (Figure 5B). The data suggests that MNDA may act as a prognostic biomarker for ALL, as its lower expression is associated with disease progression and reduced survival. The following ROC curve yielding an AUC of 0.934 (Figure 5C), demonstrating excellent predictive accuracy. In general, an AUC value above 0.9 is considered

This article is distributed under the terms of the Creative Commons Attribution-NonCommercial 4.0 International License.

[Downloaded from ijpho.ssu.ac.ir on 2026-11-25]

[DOI: 10.18502/ijpho.v15i4.19629]

highly reliable for classification, further supporting the potential of MNDA as a prognostic biomarker for ALL.

GSEA revealed that MNDA regulated the development of ALL through enrichment in multiple immune-related pathways

GSEA found that high MNDA expression in the ALL UCSC dataset was strongly associated with an enrichment in various immune-related signaling pathways, including cytokine-cytokine receptor interaction, natural killer cell-mediated cytotoxicity, Toll-like receptor signaling pathway and NOD-like receptor signaling pathway. Meanwhile, high MNDA expression was associated with apoptosis, lysosomes, complement and coagulation cascades, and hematopoietic cell lineages (common lymphoid progenitors or common myeloid progenitors) (Figure 6).

Immune infiltration analysis of tissue samples of ALL patients with high or low MNDA expression

TME includes different immune cells (23), and immune cell infiltration analysis can help us better understand tumor development (24). The immune infiltration analysis combined with CIBERSORT algorithm (Figure 7A) showed that the overall composition of immune cells had no significant difference between the two established groups, but the proportion of different immune cells had difference. The correlation analysis found a certain correlation between the immune cell components of the tissue in ALL patients (Figure 7B), but most of the correlation occurred in the same type of immune cells. The differential analysis results (Figure 8A) displayed that among the immune cell components, B cells naive, B cells memory, T cells CD4 naive, T cells follicular helper, NK cells activated, monocytes, macrophages M2 and neutrophils had significant difference between ALL patients categorized by high and low MNDA expression. Moreover, a notable correlation was witnessed between MNDA expression and immune cell components including B cells naive, T cells CD4 naive, T cells follicular helper, NK cells activated, monocytes, macrophages M2, and neutrophils (Figure 8B-H). The cells obtained from the immune cell differential analysis were intersected with those obtained from the correlation analysis, which yielded seven immune cells related to MNDA (Figure 8I). Among them, B cells naive, T cells CD4 naive, T cells follicular helper and NK cells activated were negatively correlated with MNDA expression, while monocytes, macrophages M2 and neutrophils were positively correlated with MNDA expression.

These findings imply that MNDA could be involved in immune cell infiltration in the TME of ALL patients, thereby impacting the progression of ALL.

TGIF1 might regulate MNDA expression to affect the development of ALL

To elucidate the regulatory landscape governing MNDA expression in ALL, a predictive analysis was implemented to identify potential upstream TFs involved in its modulation. First, transcriptome data of healthy AMSCs and BMSCs were extracted from GSE206172 microarray for differential analysis (Figure 9A), and 316 down-regulated DEGs in healthy BMSCs. Meanwhile, 4753 down-regulated DEGs in ALL patients were screened from the DEGs in the merged dataset of TCGA and GTEx (Figure 9B). Through the humantfs website, 1369 human TFs were downloaded and intersected with the two datasets of DEGs to obtain two TFs (MAFB, TGIF1) (Figure 9C). It has been reported that TGIF1 affected the proliferation of myeloid cells, and the absence of TGIF1 could accelerate leukemia progression and shorten survival, which indicated that TGIF1 had a

This article is distributed under the terms of the Creative Commons Attribution-NonCommercial 4.0 International License.

[Downloaded from ijpho.ssu.ac.ir on 2026-11-25]

[DOI: 10.18502/ijpho.v15i4.19629]

protective role in the development of leukemia (25).

Results from the Pearson correlation analysis uncovered a positive link between the expression of TGIF1 and MNDA in the TCGA and GTEx transcriptomic data (Figure 9D). Through the JASPAR website, the binding sites of TGIF1 (Figure 9E), and binding sites between TGIF1 and MNDA promoter regions (Table I) were predicted. Collectively, the TF TGIF1 might regulate MNDA expression, affecting the development of ALL.

Table I: Binding sites between TGIF1 and MNDA promoter region

Transcription factor	Gene Name	Start	End	Strand	Predicted sequence	Relative score
MA0796.1.TGIF1	MNDA	1909	1920	+	TGACATCTGAAA	0.81378406
MA0796.1.TGIF1	MNDA	1909	546	-	TTTCAGATGTCA	0.7874207
MA0796.1.TGIF1	MNDA	764	775	+	AGAAAGCTGTCC	0.7614015
MA0796.1.TGIF1	MNDA	536	547	-	TGCCTGCTGCCA	0.7605489

Note: TGIF1, transforming growth factor beta-induced factor homeobox 1; MNDA, myeloid nuclear differentiation antigen.

[Downloaded from ijpho.ssu.ac.ir on 2026-11-25]

[DOI: 10.18502/ijpho.v15i4.19629]

This article is distributed under the terms of the Creative Commons Attribution-NonCommercial 4.0 International License.

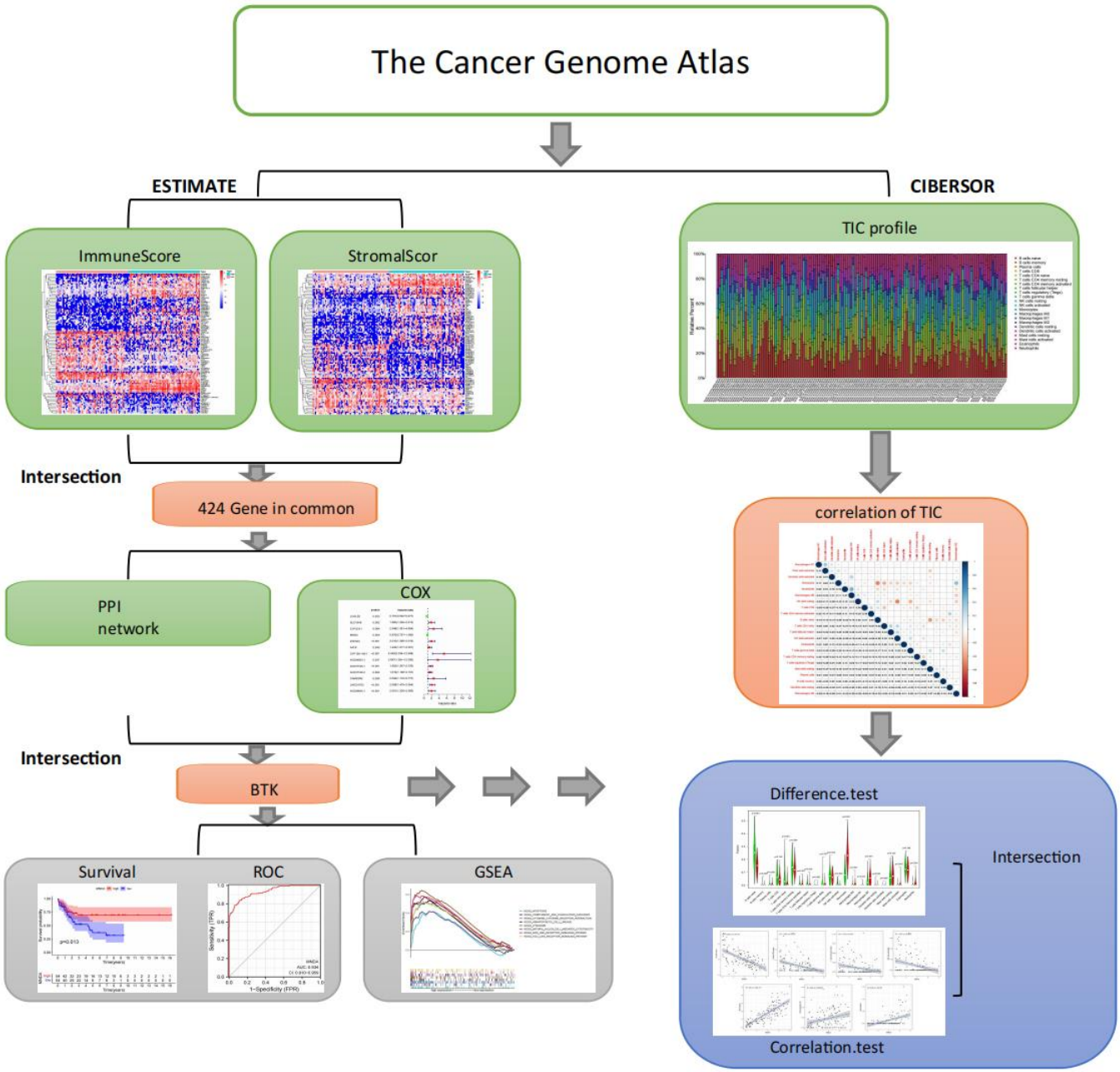

Figure 1. Schematic overview of bioinformatics analysis process.

[Downloaded from ijpho.ssu.ac.ir on 2026-11-25]

[DOI: 10.18502/ijpho.v15i4.19629]

This article is distributed under the terms of the Creative Commons Attribution-NonCommercial 4.0 International License.

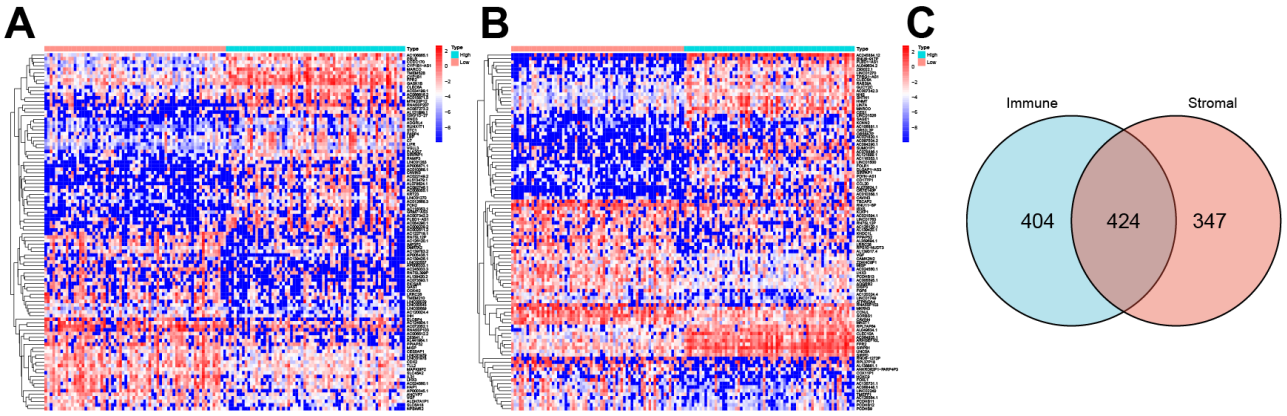

Figure 2. Identification of common DEGs in stromal and immune cells within the TME of ALL. A, Heatmap of DEGs in stromal cells in ALL gene expression dataset. B, Heatmap of DEGs in immune cells in ALL gene expression dataset. C, Venn diagram illustrating shared DEGs between stromal and immune cell populations.

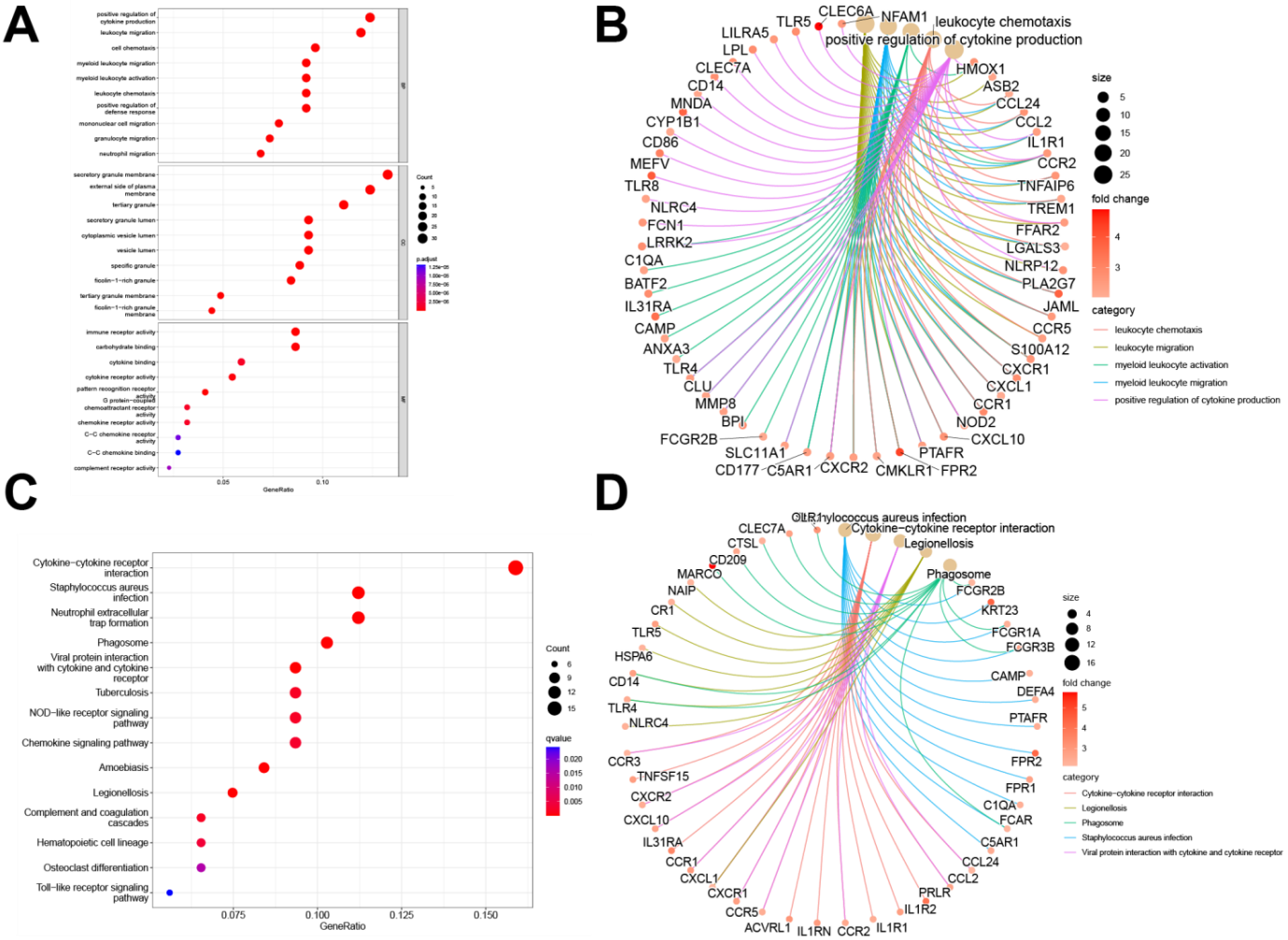

Figure 3. GO and KEGG enrichment analyses of candidate DGEs. A & B, GO function analysis of candidate DGEs in BP, CC, and MF. C & D, KEGG analysis of candidate DGEs.

This article is distributed under the terms of the Creative Commons Attribution-NonCommercial 4.0 International License.

[Downloaded from ijpho.ssu.ac.ir on 2026-11-25]

[DOI: 10.18502/ijpho.v15i4.19629]

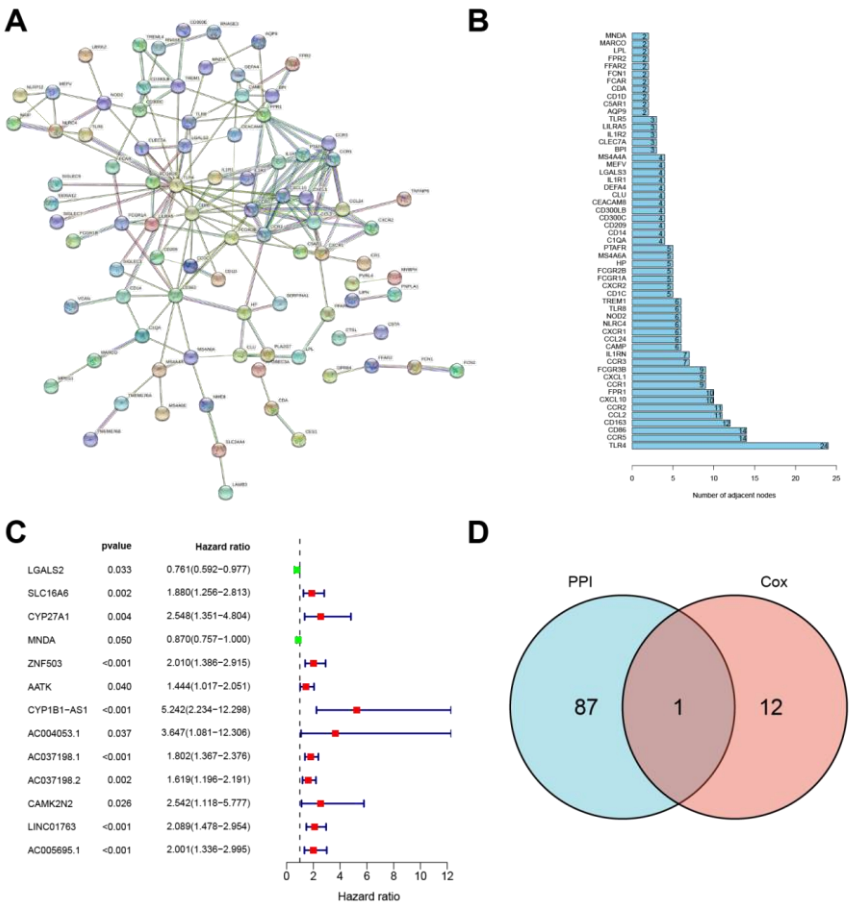

Figure 4. Identification of key genes in the TME of ALL affecting the prognosis of ALL patients. A, PPI network of candidate DGEs in ALL TME. B, Histogram of the key genes of the PPI network. C, Forest plot presenting the results of univariate Cox analysis. DEGs are listed on the left, with corresponding *p*-values shown centrally. Hazard ratios, displayed on the right, reflect the relative risk: values >1 signifies high-risk genes, while values <1 denotes low-risk genes. Gene risk status is color-coded—red for high-risk and green for low-risk candidates. D, Venn diagram depicting the overlap between hub genes identified from the PPI network and prognosis-related genes in ALL patients.

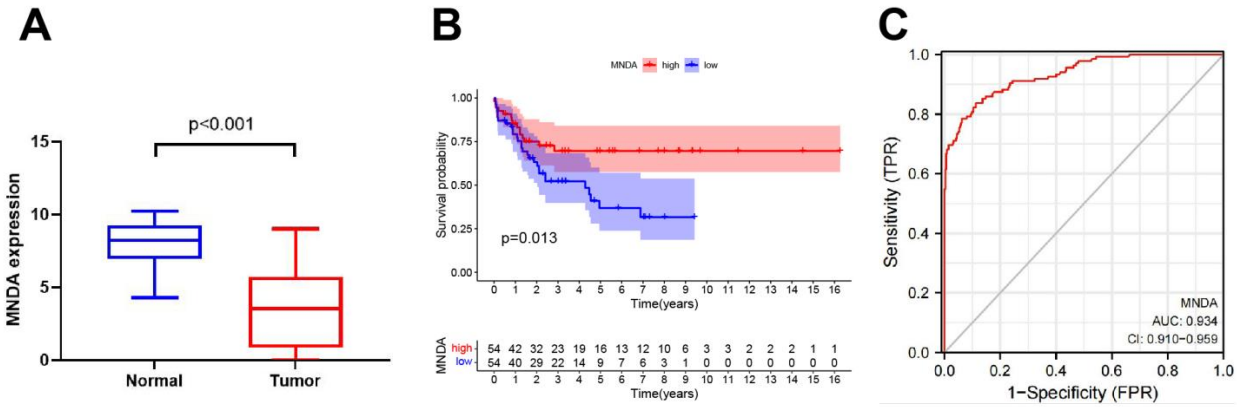

Figure 5. MNDA can significantly affect the prognosis of ALL patients. A, Single-gene differential analysis of MNDA. B, Single-gene survival analysis of MNDA. Survival probability is plotted against time. The red and blue curves correspond to high- and low-risk groups, respectively. C, ROC curve of MNDA.

This article is distributed under the terms of the Creative Commons Attribution-NonCommercial 4.0 International License.

[Downloaded from ijpho.ssu.ac.ir on 2026-11-25]

[DOI: 10.18502/ijpho.v15i4.19629]

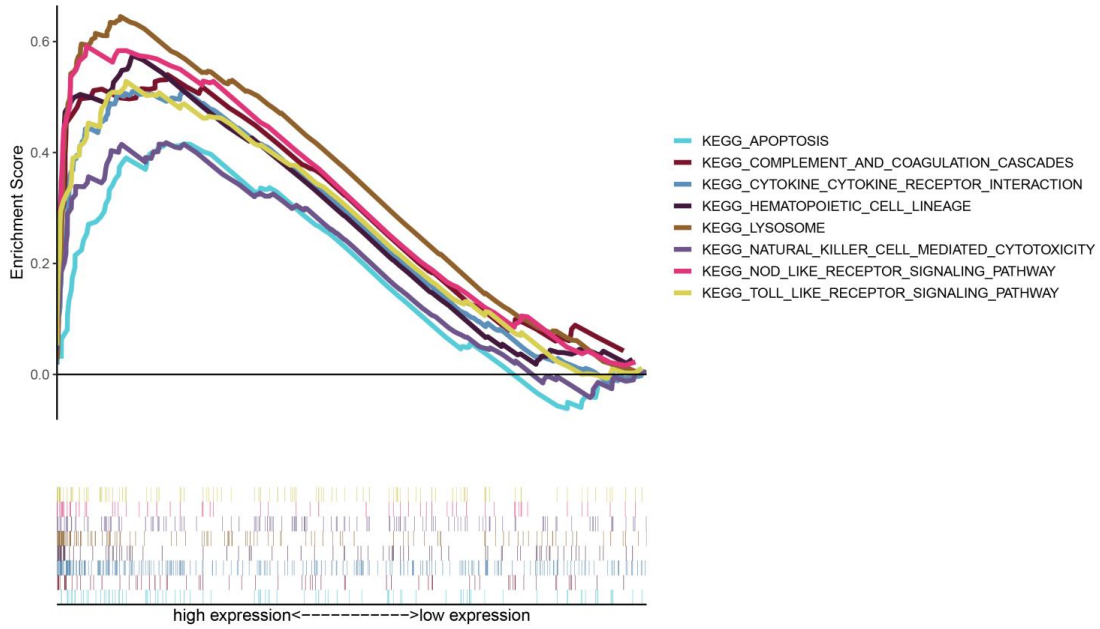

Figure 6. GSEA for the MNDA high expression group. Gene enrichment analysis of MNDA high expression in C2.kegg.v2022.1 dataset of GSEA (only immune-related data are shown).

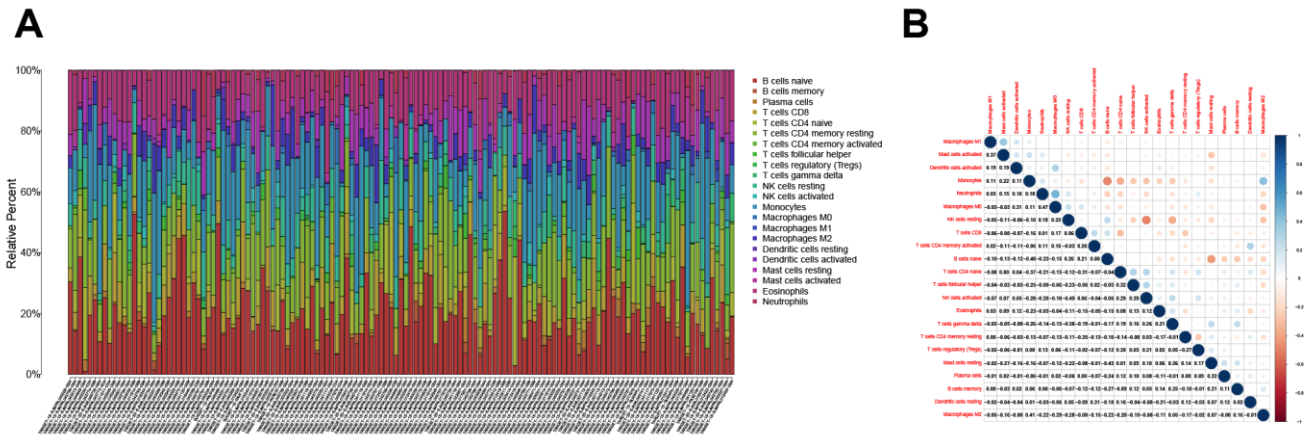

Figure 7. Immune cell component analysis and correlation analysis of ALL tissue samples in the UCSC dataset. A, Immune cell component analysis of the ALL samples. The abscissa corresponds to individual samples, while the ordinate signifies the relative abundance of immune cells. Distinct immune cell types are represented by different colors, with the color legend provided on the right. B, Immune cell correlation diagram. Each small circle indicates the pairwise correlation between two immune cell types. Positive and negative correlation coefficients are indicated by the respective color intensities, as shown in the scale bar on the right.

[Downloaded from ijpho.ssu.ac.ir on 2026-11-25]

[DOI: 10.18502/ijpho.v15i4.19629]

This article is distributed under the terms of the Creative Commons Attribution-NonCommercial 4.0 International License.

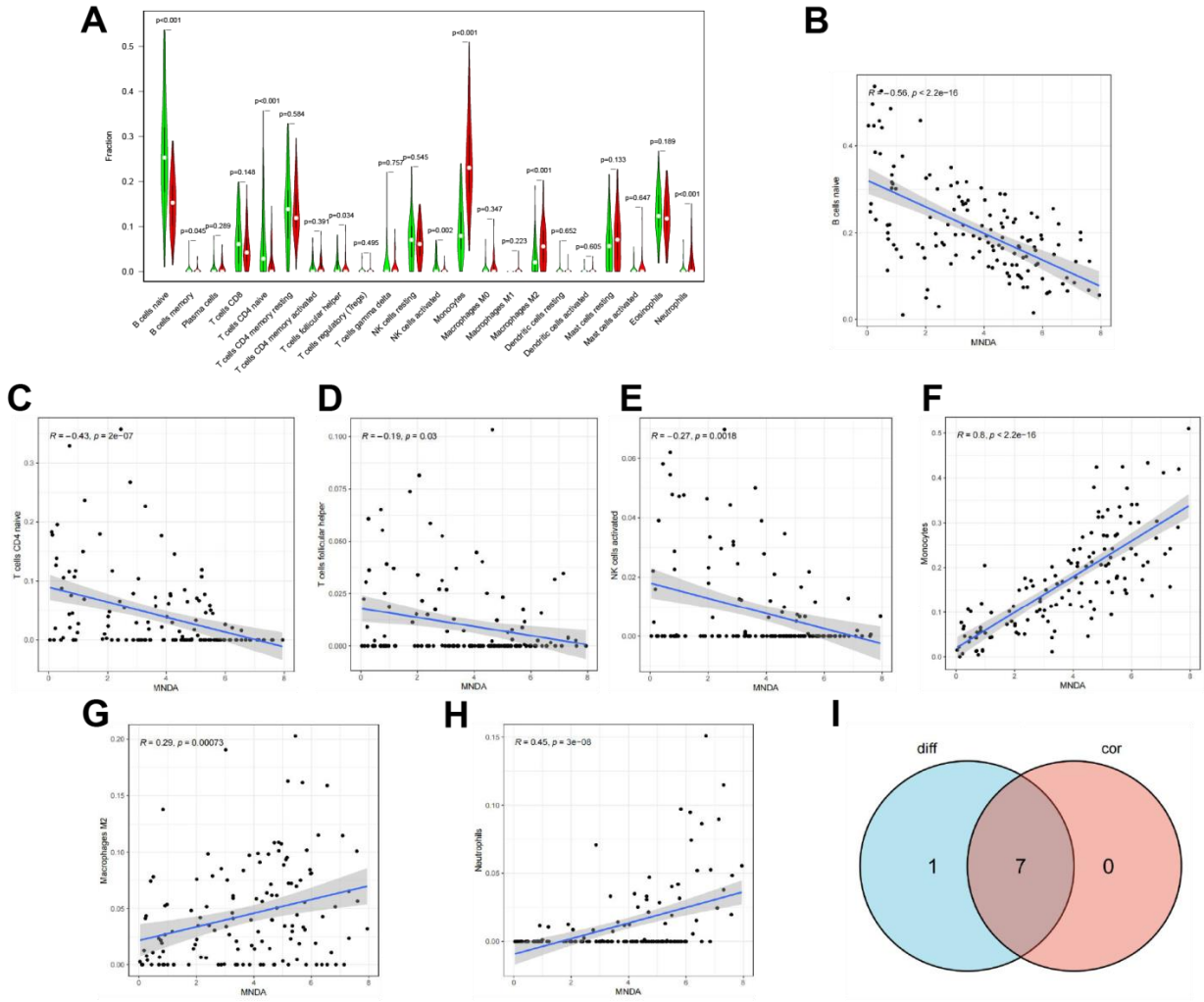

Figure 8. Identification of immune cells correlated with MNDA. A, The differential analysis of immune cell components in the high and low MNDA expression groups. Abscissa represents the immune cell type, and ordinate signifies the proportion of immune cells in the sample. Green represents low MNDA expression group, and red represents high MNDA expression group. B-H, Correlation analysis between immune cells with significantly different components [B cells naive (B), T cells CD4 naive (C), T cells follicular helper (D), NK cells activated (E), monocytes (F), macrophages M2 (G), and neutrophils (H)] and MNDA expression. Abscissa indicates MNDA expression, and ordinate indicates immune cell content. I, Venn diagram of immune cells correlated with MNDA.

[Downloaded from ijpho.ssu.ac.ir on 2026-11-25]

[DOI: 10.18502/ijpho.v15i4.19629]

This article is distributed under the terms of the Creative Commons Attribution-NonCommercial 4.0 International License.

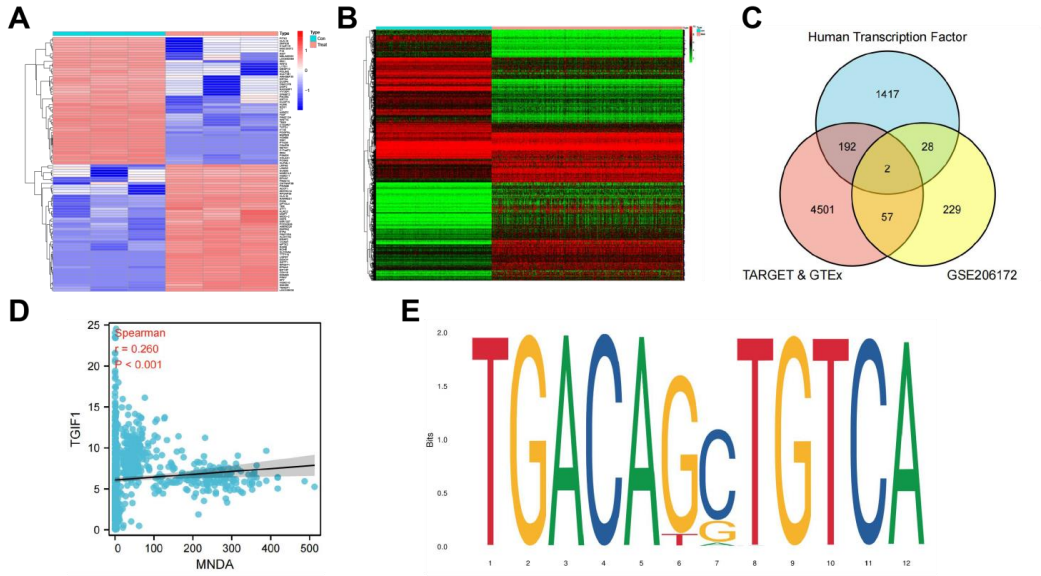

Figure 9. Prediction of transcription factors that regulate MNDA expression. A, Heatmap of the differential analysis of transcriptome data of healthy AMSCs and BMSCs extracted from GSE206172 microarray. B, Differential analysis of the merged dataset of TCGA and GTEx. C, Venn diagram summarizing the shared differentially up-regulated genes in GSE206172 microarray, differentially down-regulated genes in the merged dataset of TCGA and GTEx, and human transcription factors. D, Correlation analysis between TGIF1 and MNDA. E, The binding sites of TGIF1 predicted through JASPAR website.

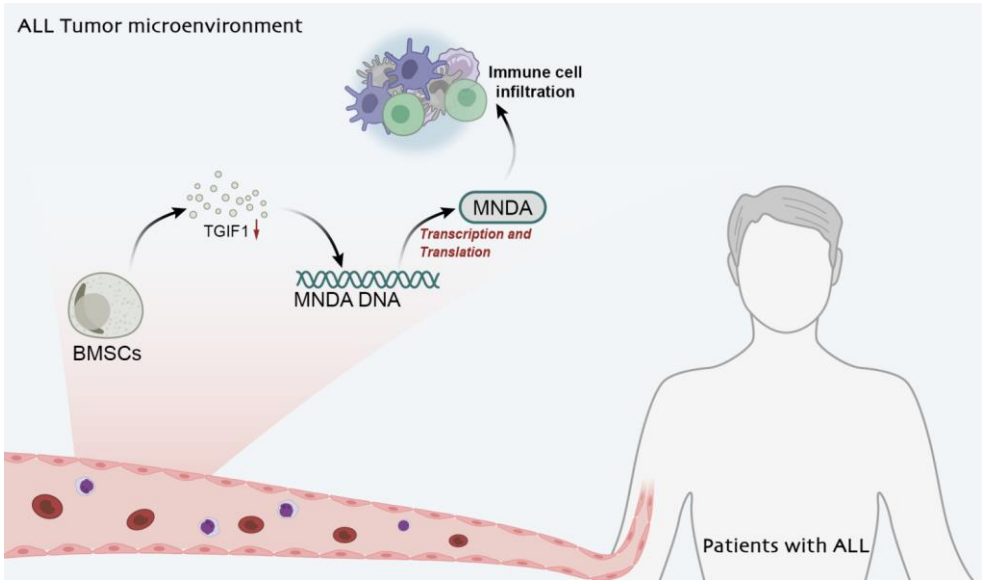

Figure 10. Schematic illustration of the molecular mechanism of BMSCs-released TGIF1 in regulating the development of ALL through MNDA. BMSCs-released TGIF1 can up-regulate the expression of MNDA, thereby inhibiting the infiltration of immune cells within the TME of ALL patients, which ultimately thwarts the development of ALL.

[Downloaded from ijpho.ssu.ac.ir on 2026-11-25]

[DOI: 10.18502/ijpho.v15i4.19629]

This article is distributed under the terms of the Creative Commons Attribution-NonCommercial 4.0 International License.

Discussion

Immune microenvironment is critical in ALL and immune-based therapeutic methods are promising for ALL treatment (26, 27). This study aimed to elucidate the mechanism by which BMSCs-derived TGIF1 regulates MNDA in the TME of ALL and its potential implications for disease progression and immune response modulation.

The results identified MNDA as a key immune-related gene within the ALL TME, with its low expression being significantly correlated with poor prognosis. MNDA was previously associated with hematopoietic differentiation and apoptosis regulation (28, 10). In CLL, MNDA has been reported as a favorable prognostic marker (29-31), where its low expression is linked to increased apoptosis resistance through MCL-1 and BCL-2 regulation (11). Expanding on these findings, the study suggests that MNDA may exert a broader immunoregulatory role in ALL, as its expression was found to be concentrated in multiple immune-related pathways.

GSEA further demonstrated that MNDA participates in cytokine-cytokine receptor interactions, chemokine signaling, and neutrophil activation, which are critical immune processes within the TME. MNDA expression showed a positive correlation with neutrophil infiltration, consistent with previous reports that MNDA is involved in neutrophil activation and immune response modulation (32, 33). This suggests that MNDA may contribute to the immunological dynamics of ALL by influencing immune cell interactions, thereby affecting disease progression. However, further mechanistic studies are required to clarify these functional roles.

In addition to identifying MNDA as a prognostic factor, the study also demonstrated that TGIF1 may serve as an upstream transcriptional regulator of MNDA. TGIF1 has been previously implicated in hematopoietic differentiation and leukemia suppression (25, 34). Notably, TGIF1 was found to be significantly upregulated in healthy BMSCs but downregulated in ALL samples, indicating a potential protective role. Prior studies have shown that TGIF1 loss accelerates leukemia progression, while its overexpression can counteract leukemia stem cell proliferation induced by IRF7 deficiency (34). Furthermore, TGIF1 expression has been identified in the vascular niche of MSCs (14), supporting its involvement in stromal-mediated leukemia regulation. These findings align with the hypothesis that BMSCs-derived TGIF1 may influence MNDA expression and contribute to immune modulation within the TME of ALL.

While this study contributes novel perspectives on MNDA in ALL, several limitations should be acknowledged. First, the computational findings were derived primarily from RNA-seq profiles of TCGA ALL tumor samples and GTEx-derived normal blood samples. Despite the relatively adequate sample size, the observed AUC of 0.934 in ROC analysis may be inflated due to potential bias arising from internal validation. Furthermore, the absence of external datasets restricts the generalizability of the results and raises concerns about possible overfitting. Future work will focus on incorporating independent cohorts to robustly assess the diagnostic and prognostic potential of MNDA. Second, the current study is largely grounded in bioinformatic inference, and the conclusions drawn require validation through functional experiments involving primary ALL specimens or animal models to substantiate the biological relevance of the findings. Third, although in silico predictions indicated that TGIF1 may act as a transcriptional regulator of MNDA via promoter binding, this regulatory

This article is distributed under the terms of the Creative Commons Attribution-NonCommercial 4.0 International License.

[Downloaded from ijpho.ssu.ac.ir on 2026-11-25]

[DOI: 10.18502/ijpho.v15i4.19629]

relationship has yet to be verified by direct molecular assays such as ChIP-seq or luciferase reporter analysis. Empirical confirmation of this interaction remains a critical next step. Lastly, the regulation of MNDA is likely multifactorial, and additional transcription factors not assessed in this study may also contribute to its expression dynamics. Future investigations should broaden the scope to identify other key regulators involved in MNDA transcriptional control.

Conclusion

In conclusion, BMSCs-released TF TGIF1 up-regulated the transcriptional expression of MNDA, thus inhibiting immune cell infiltration in the TME of ALL and ultimately suppressing the development of ALL (Figure 10). This research highlights potential molecular markers that could be pivotal for detecting and treating ALL. However, clinical samples could not be collected, and *in vivo* animal models could not be constructed for mechanistic validation, requiring further research.

Data availability

The data underlying this article will be shared on reasonable request to the corresponding author.

Ethical Considerations

This article does not contain any studies with human participants or animals experiments, and all data were obtained from publicly available databases. Ethical approval and patient consent were not required.

Acknowledgments

This study did not employ artificial intelligence (AI) techniques.

Authors' Contributions

Yibei Song: Conceptualization; Methodology; Resources; Formal analysis; Writing – original draft; Writing – review &editing.
Wienaldi: Data curation; Formal analysis; Software; Supervision; Validation; Writing – review & editing.
Maya Sari Mutia: Data curation; Formal analysis; Investigation; Writing – review & editing.

Funding

None.

Conflict of Interest

The authors declare no conflict of interest.

References

1. Tzoneva G, Perez-Garcia A, Carpenter Z, et al. Activating mutations in the NT5C2 nucleotidase gene drive chemotherapy resistance in relapsed ALL. Nat Med 2013; 19(3):368-371.
2. Duffield AS, Mullighan CG, Borowitz MJ. International consensus classification of acute lymphoblastic leukemia/lymphoma. Virchows Arch 2022; 482(1):11-26.
3. Malard F, Mohty M. Acute lymphoblastic leukaemia. The Lancet. 2020; 395(10230):1146-1162.
4. Greaves M. A causal mechanism for childhood acute lymphoblastic leukaemia. Nat Rev Cancer 2018; 18(8):471-484.
5. Terwilliger T, Abdul-Hay M. Acute lymphoblastic leukemia: a comprehensive review and 2017 update. Blood Cancer J 2017; 7(6): e577-e577.
6. Simioni C, Conti I, Varano G, Brenna C, Costanzi E, Neri LM. The Complexity of the Tumor Microenvironment and Its Role in Acute Lymphoblastic Leukemia: Implications for Therapies. Front Oncol 2021; 11-15.
7. Yu WL, Hua ZC. Identification of immune and stromal cell infiltration-related gene signature for prognosis prediction in acute lymphoblastic leukemia. Aging 2022; 14(18):7470-7504.

This article is distributed under the terms of the Creative Commons Attribution-NonCommercial 4.0 International License.

[Downloaded from ijpho.ssu.ac.ir on 2026-11-25]

[DOI: 10.18502/ijpho.v15i4.19629]

8. Gu L, Casserly D, Brady G. Myeloid cell nuclear differentiation antigen controls the pathogen-stimulated type I interferon cascade in human monocytes by transcriptional regulation of IRF7. Nat Commun 2022; 13(1):1-9.
9. Bottardi S, Layne T, Ramòn AC. MNDA, a PYHIN factor involved in transcriptional regulation and apoptosis control in leukocytes. Front Immunol 2024; 15:1-8.
10. Bellos F, Kern W. Flow cytometry in the diagnosis of myelodysplastic syndromes and the value of myeloid nuclear differentiation antigen. Cytometry Part B Clinical 2015; 92(3):200-206.
11. Bottardi S, Guieze R, Bourgoin V. MNDA controls the expression of MCL-1 and BCL-2 in chronic lymphocytic leukemia cells. Exp Hematol 2020; 88:68-82.
12. Willer A, Jakobsen JS, Ohlsson E. TGIF1 is a negative regulator of MLL-rearranged acute myeloid leukemia. Leukemia 2014; 29(5):1018-1031.
13. Yan L, Womack B, Wotton D. Tgif1 regulates quiescence and self-renewal of Hematopoietic Stem Cells. Mol Cell Biol 2013; 33(24):4824-4833.
14. Liu H, Murthi P, Qin S. A novel combination of homeobox genes is expressed in mesenchymal chorionic stem/Stromal cells in first trimester and term pregnancies. Reprod Sci 2014; 21(11):1382-1394.
15. Entrena A, Varas A, Vázquez M. Mesenchymal stem cells derived from low risk acute lymphoblastic leukemia patients promote NK cell antitumor activity. Cancer Letters 2015; 363(2):156-165.
16. Li G, Wang Y, Cai L, Zhou L. Screening for genes and subnetworks associated with atypical teratoid/rhabdoid tumors using bioinformatics analysis. Int. J. Neurosci 2020; 131(4):319-326.
17. Du Y, Miao W, Jiang X. The Epithelial to mesenchymal transition related gene calumenin is an adverse prognostic factor of bladder cancer correlated with tumor microenvironment remodeling, Gene mutation, and ferroptosis. Front Oncol 2021; 11-15.
18. Zhang D wei, Zhang S, Wu J. Expression profile analysis to predict potential biomarkers for glaucoma: BMP1, DMD and GEM. Peer J 2020; 8: e9462-9466.
19. Newman AM, Liu CL, Green MR. Robust enumeration of cell subsets from tissue expression profiles. Nat Methods 2015; 12(5):453-457.
20. Ali HR, Chlon L, Pharoah PDP, Markowetz F, Caldas C. Patterns of immune infiltration in breast cancer and their clinical implications: A Gene-expression-based retrospective study. PLoS Med 2016; 13(12): e1002194-199.
21. Cao H, Zhang Y, Chu Z, Zhao B, Wang H, An L. MAP‐1B, PACS‐2 and AHCYL1 are regulated by miR‐34A/B/C and miR‐449 in neuroplasticity following traumatic spinal cord injury in rats: Preliminary explorative results from microarray data. Mol Med Report 2019; 30:1-9.
22. Yang J. Identification of novel biomarkers, MUC5AC, MUC1, KRT7, GAPDH, CD44 for gastric cancer. Med Oncol 2020; 37(5):4-8.
23. Mierke CT. The matrix environmental and cell mechanical properties regulate cell migration and contribute to the invasive phenotype of cancer cells. Rep Prog Phys 2019; 82(6):064602-064609.
24. Kang BW, Kim JG, Lee IH, Bae HI, Seo AN. Clinical significance of tumor-infiltrating lymphocytes for gastric cancer in the era of immunology. WJGO 2017; 9(7): 293-299.
25. Yan L, Davé UP, Engel M, Brandt SJ, Hamid R. Loss of TG-Interacting Factor 1 decreases survival in mouse models of myeloid leukaemia. J Cellular

This article is distributed under the terms of the Creative Commons Attribution-NonCommercial 4.0 International License.

[Downloaded from ijpho.ssu.ac.ir on 2026-11-25]

[DOI: 10.18502/ijpho.v15i4.19629]

Molecular Medi 2020; 24(22):13472-13480.
26. Witkowski MT, Dolgalev I, Evensen NA. Extensive remodeling of the immune microenvironment in B Cell acute lymphoblastic leukemia. Cancer Cell 2020; 37(6):867-882.
27. Jiménez-Morales S, Aranda-Uribe IS, Pérez-Amado CJ, Ramírez-Bello J, Hidalgo-Miranda A. Mechanisms of immunosuppressive tumor evasion: Focus on acute lymphoblastic leukemia. Front Immunol 2021; 12-17.
28. Fotouhi-Ardakani N, Kebir DE, Pierre-Charles N. Role for myeloid nuclear differentiation antigen in the regulation of neutrophil apoptosis during sepsis. Am J Respir Crit Care Med 2010; 182(3):341-350.
29. Joshi AD, Hegde GV, Dickinson JD. ATM, CTLA4, MNDA, andHEM1in High versus low CD38–expressing B-Cell Chronic Lymphocytic Leukemia. Clin Canc Res 2007; 13(18):5295-5304.
30. Mittal AK, Hegde GV, Aoun P. Molecular basis of aggressive disease in chronic lymphocytic leukemia patients with 11q deletion and trisomy 12 chromosomal abnormalities. Int J Mol Med 2007; 20(4):461-469.
31. Kanellis G, Roncador G, Arribas A. Identification of MNDA as a new marker for nodal marginal zone lymphoma. Leukemia 2009; 23(10):1847-1857.
32. Chu Y, Yu F, Wu Y. Identification of genes and key pathways underlying the pathophysiological association between nonalcoholic fatty liver disease and atrial fibrillation. BMC Med Genomics 2022; 15(1):1-8.
33. Zhao J, Zhang X, Guan J, Su Y, Jiang J. Identification of key biomarkers in steroid-induced osteonecrosis of the femoral head and their correlation with immune infiltration by bioinformatics analysis. BMC Musculoskelet Disord 2022; 23(1):4-9.
34. Wang H, Zhang D, Cui X. Loss of IRF7 accelerates acute myeloid leukemia progression and induces VCAM1-VLA-4 mediated intracerebral invasion. Oncogene 2022; 41(16):2303-2314.

[Downloaded from ijpho.ssu.ac.ir on 2026-11-25]

[DOI: 10.18502/ijpho.v15i4.19629]

This article is distributed under the terms of the Creative Commons Attribution-NonCommercial 4.0 International License.